NJC

Accepted Manuscript

This is an *Accepted Manuscript*, which has been through the Royal Society of Chemistry peer review process and has been accepted for publication.

Accepted Manuscripts are published online shortly after acceptance, before technical editing, formatting and proof reading. Using this free service, authors can make their results available to the community, in citable form, before we publish the edited article. We will replace this *Accepted Manuscript* with the edited and formatted *Advance Article* as soon as it is available.

You can find more information about *Accepted Manuscripts* in the Information for Authors.

Please note that technical editing may introduce minor changes to the text and/or graphics, which may alter content. The journal's standard Terms & Conditions and the Ethical guidelines still apply. In no event shall the Royal Society of Chemistry be held responsible for any errors or omissions in this *Accepted Manuscript* or any consequences arising from the use of any information it contains.

ROYAL SOCIETY OF CHEMISTRY

www.rsc.org/njc

NJC

RSCPublishing

PAPER (or FOCUS or PERSPECTIVE)

Double Bond Terminated Ln^{3+}-doped $LiYF_4$ Nanocrystals with Strong Single Band NIR Emission: Simple Click Chemistry Route to Make Water Dispersible Nanocrystals with Various Functional Groups

Cite this: DOI: 10.1039/c3nj00000x

Received 00th XXXXX 2013,
Accepted 00th XXXXX 2013

DOI: 10.1039/c3nj00000x

www.rsc.org/njc

Brahmaiah Meesaragandla[a], Debasrita Sarkar[a], Venkata N. K. B. Adusumalli[a] and Venkataramanan Mahalingam[a*]

We have developed a versatile and simple strategy for converting hydrophobic upconverting nanocrystals into water dispersible with a variety of functional groups at the surface using thiol-ene click chemistry. This is achieved by covalently linking thiol groups containing molecules such as cysteine, cysteamine, 3-mercaptopropanoic acid and 2,3 dimercapto-1-propanol to undecenoic acid capped Yb^{3+}/Tm^{3+} doped $LiYF_4$ nanocrystals via click chemistry in the presence of azobisisobutyronitrile (AIBN). This method allows provision to place variety of functional groups at the surface of the nanocrystals. The shape and size of the nanocrystals were preserved even after surface modification. Interestingly, the undecenoic acid capped Yb^{3+}/Tm^{3+} doped $LiYF_4$ nanocrystals show strong emission in the NIR region compared to emissions in the visible region.

Introduction

The lanthanide (Ln^{3+}) ions doped nanocrystals with strong upconversion property have been attracted a wide scientific interest due to their range of applications, such as photodynamic therapy[1-2], nano-thermometry[3], drug delivery[4],bioimaging, just to mention a few [5-10] This is due to their ability in converting two or more photons of lower energy (NIR) into one higher energy photon in the visible region via nonlinear multiphoton process.[11-19] Materials showing NIR-to-NIR upconversion luminescence find interesting for bioimaging application as both excitation and emitted radiations fall in the biological transparent window (700−1000 nm). These materials have remarkable luminescence properties such as narrow band width, absence of autofluorescence, low toxicity and high contrast in bio imaging due to deep penetration of light into tissues.[3]

The interest in fluoride nanocrystals stems from the low phonon energy (400 cm^{-1}) and the wide availability of different synthetic methods to prepare them. Thermal decomposition method is one of the widely studied method to make fluoride nanocrystals. In this method, Ln^{3+}-trifluoroacetate precursors are decomposed at high temperature and the choice of stabilizing ligands is generally limited to oleic acid (OA), and oleylamine.[20-21] One of the major advantage of upconverting nanocrystals is their use in bioimaging applications. This demands that the nanocrystals need to be stable in biological medium. This motivates several groups to develop synthetic strategy to make water dispersible nanocrystals.

Post surface chemical modification is one of the strategies to tune the surface properties of the materials.[22] There are quite a few works on post chemical methods to convert hydrophobic Ln-doped nanocrystals into hydrophilic ones. For example, oxidation of the double bond in OA capped nanocrystals using Lemieux–von Rudloff reagent ($KMnO_4/NaIO_4$).[23] This process leads to the formation of carboxylic acid groups at the end, thus making the nanocrystals water dispersible. Second approach is the epoxidation of the double bond using 3-chloroperoxybenzoic acid and ring opening with cysteine and polyethylene glycol monomethyl ether.[24] The above reactions usually takes long time for the completion of the reaction due to the steric hindrance for the reagents to reach the double bond which is present between the long aliphatic chains. Recently our group used simple hydroxylation technique to convert hydrophobic $BaLuF_5$:Yb/Er nanocrystals into water dispersible.[25] In this method ricinoleic acid was used as capping agent, which has one OH group near the double bond. Hydroxylation was achieved by epoxidation of double bond with H_2O_2/HCOOH and ring opening by NaOH. The presence of three OH groups renders the nanocrystals water dispersible. This reaction was relatively faster and takes about 8 h to complete. Most of the surface functionalization methods takes long reaction time and provides only one functional group on the surface

of the nanocrystals. In addition, bioanalytical applications require a functional group on the surface of the upconverting nanocrystals to specifically bind cellular target structures or other analytes. Our idea is to explore thiol-ene click reaction, as is one of the easily accessible platform for converting the hydrophobic nanocrystals into water dispersible with a variety of functional groups on the surface of the upconverting nanocrystals.

In this work, we used 10-undecenoic acid (UDA) as stabilizing ligand in the synthesis of Yb^{3+}/Tm^{3+} doped $LiYF_4$ upconverting nanocrystals as well as to make the nanocrystal surface hydrophilic. The presence of the double bond at the surface of the nanocrystals easily assists the thiol-ene functionalization with various thiol group containing molecules such as cysteine, cysteamine 3-mercapto propanoic acid (MPA) and 2,3 dimercapto-1-propanol (DMP). This led to the presence of different functional groups at the surface such as COOH, NH_2 and OH thus making the nanocrystals surface hydrophilic. The average size, shape and phase of the nanocrystals are preserved after thiol-ene modification. After surface modification the nanocrystals are water dispersible and displayed strong emission in the NIR region via upconversion process.

Results and Discussion

The Yb^{3+}/Tm^{3+}(27/0.5%) doped $LiYF_4$ nanocrystals (NCs) were prepared using thermal decomposition method (see experimental section).[26] Figure 1a shows the X-ray diffraction (XRD) results of the UDA capped Yb^{3+}/Tm^{3+} doped $LiYF_4$ NCs. The diffraction peak positions and relative intensities of the NCs are in good agreement with the standard pattern of tetragonal phase bulk $LiYF_4$. Figure 1b shows the TEM image of the UDA capped Yb^{3+}/Tm^{3+} doped $LiYF_4$ NCs. The NCs possess diamond shaped morphology with an average aspect ratio (length/breadth) ~1.2. Inset in Figure b shows the high resolution TEM image of a nanocrystal where the lattice arrangement of atoms is clearly visible. The high dispersibility of the NCs in toluene indicates the attachment of UDA to the surface of the NCs. The strong attachment of UDA to the NCs is further verified by FTIR analysis. Figure 2 shows the FTIR spectra of pure UDA and UDA capped Yb^{3+}/Tm^{3+} doped $LiYF_4$ NCs. The peak observed near 1718 cm^{-1} for pure UDA due to C=O stretching of COOH group is shifted to 1550 and 1450 cm^{-1} upon

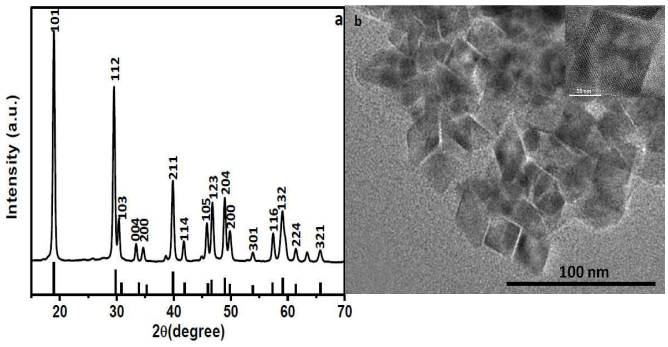

Figure 1. a) XRD pattern and b) TEM image of UDA capped Yb^{3+}/Tm^{3+} doped $LiYF_4$ NCs. The vertical lines in (a) is the standard pattern for the tetragonal bulk $LiYF_4$.

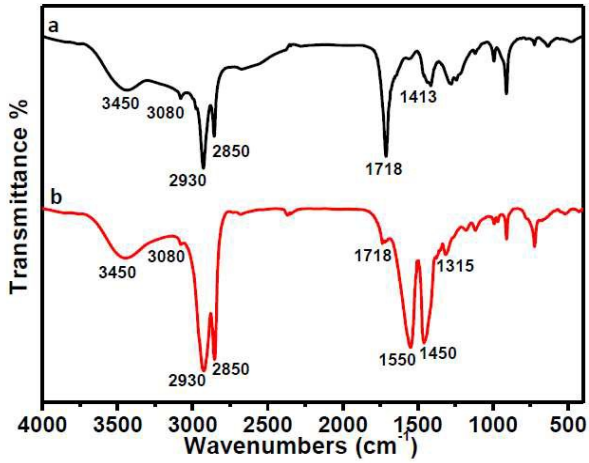

Figure 2. FTIR spectra of a) pure UDA and b) UDA capped Yb^{3+}/Tm^{3+} doped $LiYF_4$ nanocrystals.

binding to the NCs. These peaks are assigned to the asymmetric and symmetric stretching frequencies of COO^- group. The band observed at 3080 cm^{-1} in pure UDA as well as in UDA capped Yb^{3+}/Tm^{3+} doped $LiYF_4$ NCs is assigned to C-H stretching of $HC=CH_2$ group. The attachment of UDA to the NCs is further supported by ^{1}H-NMR analysis. Figure S1 and S2 show the ^{1}H-NMR spectra of pure UDA and UDA capped Yb^{3+}/Tm^{3+} doped $LiYF_4$ NCs. The peaks (multiplet) between 4.91-5.81 ppm due to the protons in the $CH=CH_2$ group present in pure UDA as well as after binding to the nanocrystals.

Figure 3 shows the upconversion emission spectrum of the UDA capped Yb^{3+}/Tm^{3+} doped $LiYF_4$ NCs in toluene. Upon 980 nm excitation, Tm^{3+}/Yb^{3+}-doped $LiYF_4$ NCs show intense emission at 790 nm, in addition to very weak peaks at 450, 650nm. Due to high absorption coefficient, the Yb^{3+} ions act as efficient sensitizer for the Tm^{3+} ions. The origin of these emissions is from the excited energy levels of Tm^{3+} ions, which

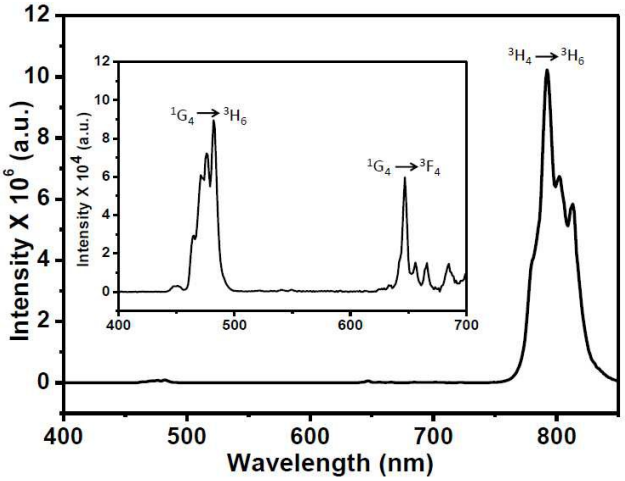

Figure 3. Upconversion emission spectrum of the UDA capped Yb^{3+}/Tm^{3+} doped $LiYF_4$ NCs in toluene (0.5 wt %). Inset shows the emissions in the visible region (enlarged region).

are populated by multiple energy transfers from excited Yb^{3+} ions. The blue emission band observed at 480 nm, is due to

$^1G_4 \rightarrow {}^3H_6$ transitions of Tm^{3+} ions, and the red emission at 645 nm is assigned to $^1G_4 \rightarrow {}^3F_4$ transition. The strong emission peak observed at 790 nm is ascribed to $^3H_4 \rightarrow {}^3H_6$ transition of Tm^{3+} ions. We emphasize that the observed emission pattern is quite different from that obtained for $LiYF_4$:Yb^{3+}/Tm^{3+} NCs.[27-29] Thereare reports that increased amount of Yb^{3+} ions in the NCs will increase the ratio of NIR to blue emission. In fact, we and others have shown that in Tm^{3+}/Yb^{3+}-doped $NaYF_4$ and $LiYbF_4$ NCs, strong NIR emission is noted compared to the blue emission near 480 nm.[30-31] As increased Yb^{3+} ion concentration in the matrix might lead to back energy transfer (from Tm^{3+} to Yb^{3+} levels), we slightly increase the Yb^{3+} ion concentration (to 27%) and observed an increase in the NIR to blue emission ratio. Single band NIR emission is advantageous as NIR light is silent to tissues and can improve the contrast in the imaging process.

To take advantage of the double bond at the surface of the NCs, we performed thiol-ene click reaction with various molecules containing different functional groups. We choose cysteine, cysteamine, MPA and DMP molecules such that the resulting NCs will have COOH, NH_2, OH fucntional groups at the terminal. This one step reaction was achieved by simple heating of the mixture containing thiol group molecules and alkene terminated Yb^{3+}/Tm^{3+} doped $LiYF_4$ NCs in the presence of thermal intiator AIBN. The mechanism involved in this reaction is the formation of radicals (thiol and alkene) in the presence of AIBN followed by the addition of these moieties. A schematic illustration of surface modification with different molecules is shown in scheme 1.

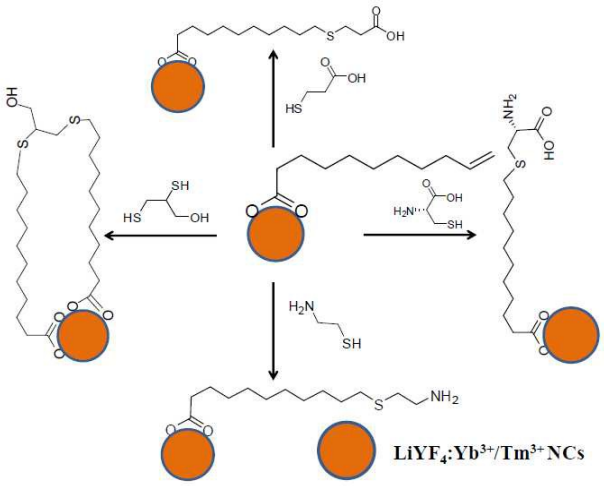

Scheme 1. Schematic illustration of the surface modification of UDA capped Yb^{3+}/Tm^{3+} doped $LiYF_4$ NCs using thiol-ene chemistry.

To confirm the attachment of thiols to the double bonds we have performed FTIR analysis after the surface reaction. Figure 4 shows the FTIR spectra of UDA capped Yb^{3+}/Tm^{3+} doped $LiYF_4$ NCs after thiol-ene modification with cysteine,

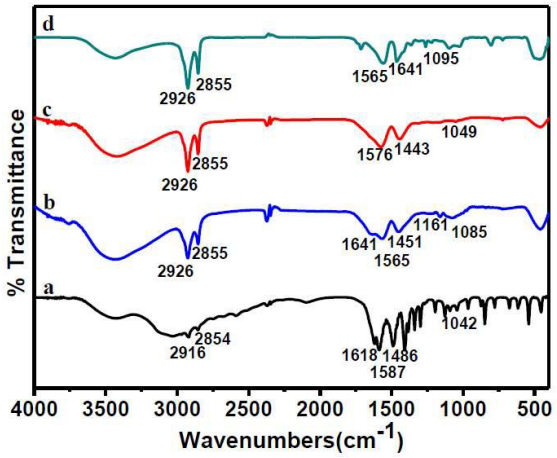

Figure 4. FTIR spectra of UDA capped Yb^{3+}/Tm^{3+} doped $LiYF_4$ NCs after thiol-ene modification with a) cysteine b) cysteamine c) MPA and d) DMP.

cysteamine, MPA and DMP. In the case of cysteine modified NCs, the band observed near 1618 cm^{-1} is attributed to the carbonyl (C=O) vibrational stretching frequency and the two bands at 1587 and 1042 cm^{-1} are assigned to N-H flexural vibration and C-N stretching vibration, respectively. For cysteamine modified NCs the bands observed near 1641 and 1085 cm^{-1} assigned to the N-H bending vibration and C-N stretching vibration, respectively. For MPA modified NCs, the C=O stretching frequency of free COOH group is masked by the broad 1576 cm^{-1} peak. In case of DMP coated NCs, the peak observed at 1095 cm^{-1} is assigned to the C-O stretching of C-OH bond. The presence of new bands and the absence of characteristic band of C-H stretching peak of $-HC=CH_2$ at 3077 cm^{-1} suggest that thiol-ene modification was performed successfully.

Figure 5 shows the upconversion luminescence of Yb^{3+}/Tm^{3+} doped $LiYF_4$ NCs in water after thiol-ene modifications with cysteine, cysteamine, MPA and DMP. Among which MPA and DMP modified NCs show intense upconversion emission compared to cysteine, cysteamine modified NCs. The observed difference in the emission intensity between the NCs after surface modification is not due to difference in size of the NCs. This fact is confirmed by performing DLS analysis for the NCs after thiol-ene reaction. The DLS results suggest there is only a slight difference in the average hydrodynamic radius between the four NCs after surface modifications (see Figure S3 in supporting information). In general, the upconversion efficiency of Ln^{3+} ion doped NCs is strongly influenced by the surface properties of the NCs. The upconversion efficiency can be strongly reduced if the groups with high energy vibrational modes i.e OH-, NH_2- are located near the Ln^{3+} ions. Hence the surface ligands and the solvent molecules strongly affect the optical properties of these NCs. We believe the difference in the observed intensity pattern may be due to the availability of -COOH and –OH groups on the surface of the NCs which effectively make hydrogen bonding with the water molecules compared to NH_2 groups (cysteine, cysteamine). It is reasonable that even though OH-

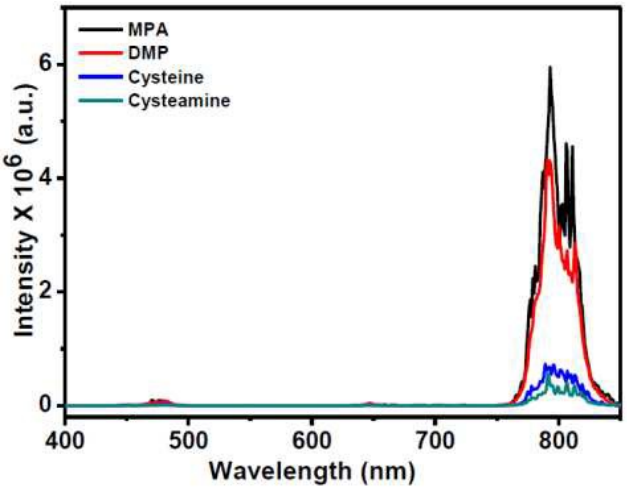

Figure 5. Upconversion emission spectra of UDA capped Yb^{3+}/Tm^{3+} doped $LiYF_4$ NCs in water (0.5 wt%) after thiol-ene modification with cysteine, cysteamine, MPA and DMP.

group has high energy stretching frequency, it effectively makes hydrogen bonding with the water molecules compared to NH_2 groups, thus barely affects the upconversion efficiency. In the case of cysteine and cysteamine coated NCs, NH_2 groups present on the surface of the NCs quench the luminescence due to their high energy stretching frequencies.

A time dependent upconversion emission analysis was performed to understand how stable these NCs are in water after surface modification. It is clear from the emission spectra shown in Figure S4 (see supporting information), Yb^{3+}/Tm^{3+} doped $LiYF_4$ NCs after thiol-ene reaction, are quite stable. This is due to the availability of free -COOH,–OH and -NH_2 functional groups. The relatively higher emission intensity noted in the case of MPA and DMP modified nanocrystals is presumable due to extra stabilization achieved through weak interactions such as hydrogen bonding. The slight decrease in the intensity over time in all the nanocrystals is likely due to the slow settling of the NCs caused by the hydrophobic interactions between the methylene groups in UDA.

To investigate the effect of dispersion medium (water) on the emission, we have performed luminescence measurements in D_2O. Figure S5 shows the upconversion emission spectra of the cysteine, cysteamine, MPA and DMP coated $Yb^{3+/}Tm^{3+}$ doped $LiYF_4$ NCs in D_2O. The emission spectra of the Yb^{3+}/Tm^{3+} doped $LiYF_4$ NCs in D_2O are quite intense compared to the ones from the same sample dispersed in H_2O. We presume this is due to the isotope effect, which reduce the nonradiative pathways in the multiphonon deactivation process since the OD oscillators are relatively less efficient compared to OH.[32]

To understand the effect of different polar solvents on the emission, we have performed luminescence measurements in DMSO, DMF and ethanol. Figure S6 shows the upconversion emission spectra of the cysteine, cysteamine, MPA and DMP coated Yb^{3+}/Tm^{3+} doped $LiYF_4$ NCs in DMSO, DMF and ethanol. It is evident from the spectra that the Yb^{3+}/Tm^{3+} doped $LiYF_4$ NCs in DMSO, DMF and ethanol are more or less similar except for the slight differences in the blue to NIR emission ratio. To get more insight, we have calculated the blue/NIR emission intensities for the four samples in different solvents. A comparison is made and shown in Table S1, ESI). It is clear there is slight increase in the blue/NIR emission ratio in DMSO compared to polar solvents like water and ethanol. Though the exact reason is not clear, we believe that solvents and their polarity play a major role in controlling the non-radiative decay pathways which result in the slight difference in the ratio between the peaks. It is likely that the functional groups at the surface of the nanocrystals or their orientation control the diffusion of solvent molecules reaching the surface of the nanocrystals. This alters the solvation sphere around the nanocrystals surface.

To confirm that the phase of the NCs is preserved after thiol-ene modification with cysteine, cysteamine, MPA and DMP, XRD measurements were done. The XRD patterns shown in Figure 6 (*vide infra*) match with the UDA capped Yb^{3+}/Tm^{3+} doped $LiYF_4$ NCs, conforming that the phase of the NCs is not affected after thiol-ene reaction.

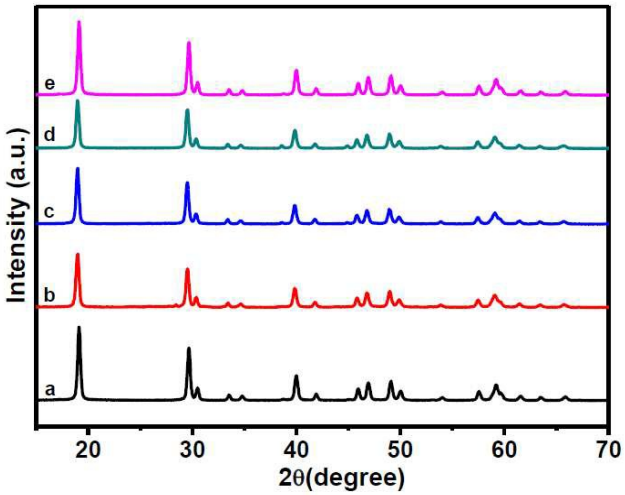

Figure 6. PXRD patterns of a) UDA capped Yb^{3+}/Tm^{3+} doped $LiYF_4$ NCs and after thiol-ene modification with b) cysteine c) cysteamine d) MPA e) DMP.

Conclusions

In conclusion, we have shown a simple chemical approach to convert hydrophobic upconverting NCs into hydrophilic one using thiol-ene click chemistry. The undecenoic acid capped Yb^{3+}/Tm^{3+} doped $LiYF_4$ NCs have double bonds at the surface of the NCs, which provides easy accessibility for the thiol group containing molecules such as cysteine, cysteamine, 3-mercaptopropanoic acid and 2,3 dimercapto-1-propanol to react with the double bond via thiol-ene click chemistry. The nanocrystals after surface modification are quiet stable in water as well as in other polar solvents. Both phase and the optical properties of the NCs are preserved after surface modifications. This method is quite advantageous as this allows one to prepare upconverting nanocrystlas with variety of functional moieties. The small size, high polar dispersibility with different functionality and strong NIR to NIR upconversion emission

from the NCs can be utilized for in vivo deep tissue biomedical imaging.

Experimental

Materials

Rare earth oxides of high purity Y_2O_3, Yb_2O_3, Tm_2O_3 and CF_3COOLi, 10-undecenoic acid (UDA), 1-octadecene (90%), $CDCl_3$, azobisisobutyronitrile (AIBN), 2,3-dimercapto-1-propanol (DMP), 3- mercaptopropanoic acid (MPA), cysteine hydrochloride and cysteamine hydrochloride were purchased from Sigma-Aldrich. Ethanol, trifluoroacetic acid, toluene, cyclohexane, dichloromethane and hexane were purchased from Merck. All chemicals were used without further purification.

Synthesis of UDA capped Yb^{3+}/Tm^{3+} doped $LiYF_4$ NCs

The Yb^{3+}/Tm^{3+} doped $LiYF_4$ NCs were synthesized using the thermal decomposition method.[26] In brief, a mixture of 0.725 mmol Y_2O_3, 0.27 mmol Yb_2O_3, and 0.005 mmolTm_2O_3 in 5 mL trifluoroacetic acid and 5 mL of distilled water were taken in a three necked flask and reflexed at 85^o C until clear solution was obtained. The resulting solution was evaporated to dryness. Subsequently 2.5 mmol CF_3COOLi was added to the flask along with 4 g of 10-undecenoic acid, and 20 ml of 1-octadecene. The slurry was degassed and heated to 120 ^{o}C with vigorous magnetic stirring for 30 min to remove water and oxygen. Subsequently, the mixture was heated to 300 ^{o}C at a heating rate of 20 ^{o}C/min under the Ar atmosphere. The solution became a bit turbid and was maintained at this temperature for 1 h under Ar atmosphere. Next, the mixture was left to cool in air with gentle stirring. Then, the resultant mixture was precipitated by adding an excess amount of ethanol into the mixture and the products were collected by centrifugation. The as-precipitated NCs were washed several times with hexane and ethanol, and then dried for 24 h.

Cysteine and cysteamine modified Yb^{3+}/Tm^{3+} doped $LiYF_4$ NCs

Cysteine hydrochloride (70 mg) water solution (10 mL) and AIBN (10 mg)-ethanol solution (10 mL) were added to the as-prepared UDA capped Yb^{3+}/Tm^{3+} doped $LiYF_4$ NCs (50 mg) dispersed in 15 ml of cyclohexane:DCM (2:1) solution at room temperature. The mixture was heated to 60 °C and maintained for 3 h under Ar flow to modify UDA capped Yb^{3+}/Tm^{3+} doped $LiYF_4$ NCs with cysteine via the thiol-ene click reaction. Then the mixture was allowed cool to room temperature and the cysteine coated Yb^{3+}/Tm^{3+} doped $LiYF_4$ NCs was collected by centrifugation and washed with water several times. Similar procedure was followed for cysteamine capped NCs.

MPA and DMP modified Yb^{3+}/Tm^{3+} doped $LiYF_4$ NCs

0.3 ml, MPA and AIBN (10 mg)-ethanol solution (10 mL) were added to the as-prepared UDA capped Yb^{3+}/Tm^{3+} doped $LiYF_4$ NCs (50mg) dispersed in 15 ml of cyclohexane:DCM (2:1) solution at room temperature. The mixture was heated to 60 °C and maintained for 3 h under Ar flow to modify UDA capped Yb^{3+}/Tm^{3+} doped $LiYF_4$ NCs with MPA via the thiol-ene click reaction. Then allowed the mixture to room temperature and collect the MPA coated Yb^{3+}/Tm^{3+} doped $LiYF_4$ NCs by centrifugation and washed with water several times. Similar procedure was followed for DMP capped NCs.

Characterization

The X-ray diffraction (XRD) patterns of the UDA capped NCs were acquired using a Rigaku-SmartLab X-ray diffractometer with D/texultra detector and Cu K_α source operating at 70 kV and 35 mA. The scan range was set from 10° to 70° with a step size of 0.028 and a count time of 2 s. The samples were ground completely and spread evenly on a quartz slide. The size and morphology of the NCs were obtained from FEI Technai G2 UTwin (200 keV) TEM instrument. Samples were prepared by placing a drop of dilute toluene dispersion for UDA capped NCs. FTIR spectra were acquired with a PerkinElmer FTIR spectrometer 1000 with a resolution of 2 cm^{-1}. The solid samples were taken as dry powder and pelletized with KBr, and the pellets were placed on the sample holder. The ^1H -NMR spectra of pure UDA, UDA capped Yb^{3+}/Tm^{3+} doped $LiYF_4$ NCs dispersed in $CDCl_3$ were recorded on a JEOL 400 MHz spectrometer. Upconversion measurements were done by exciting the 0.5 wt% nanocrystal dispersion with a 980 nm diode laser from RgBLase LLC, which was coupled to a fiber with core diameter of 100 µm. The emitted light was detected using a Horiba JobinYvon fluorimeter equipped with a photomultiplier tube. To remove the scattered excitation light, a long-band pass filter (495 nm) was used on the excitation side. All upconversion emission spectra were measured with the same slit width at the same excitation laser power of 500 mW. Zeta potential and DLS measurements were measured using a Malvern Zetasizer nano equipped with a 4.0 mW He-Ne laser operating at λ=630nm. All samples were measured in an aqueous system at room temperature with scattering angle of 173°. Size distribution calculated by nano software is derived from a non negative least square (NNLS) analysis

Acknowledgements

V.M. thanks CSIR for the project 01(2716)13 and the Indian Institute of Science Education and Research (IISER), Kolkata, for the funding. B.M, D.S and V.N.K.B.A thank IISER Kolkata and UGC, respectively, for funding.

Notes and references

a Indian Institute of Science Education and Research (IISER) Kolkata, Mohanpur, Nadia district 741246, West Bengal.
*Corresponding author; mvenkataramanan@yahoo.com

Electronic Supplementary Information (ESI) available: [DLS results, NMR spectra of nanocrystals, time-dependent upconversion spectra]. See DOI: 10.1039/b000000x/

1. G. Tian, W. Ren, L. Yan, S. Jian, Z. Gu, L. Zhou, S. Jin, W. Yin, S. Li, Y. Zhao, *Small* 2013, **9**, 1929–1938.

2. N. M. Idris, M. K. Gnanasammandhan, J. Zhang, P. C. Ho, R. Mahendran, Y. Zhang, *Nat. Med.* 2012, **18**, 1580-1586.
3. (a) L. D. Carlos, R. A. Sá Ferreira, V. de Zea Bermudez, S. J. L. Ribeiro, *Adv. Mater.* 2009, **21**, 509-534; (b) D. S. Brites, P. P. Lima, N. J. O. Silva, A. Millán, V. S. Amaral, F. Palacio, L. D. Carlos, *New J. Chem.* 2011, **35**, 1177–1183; (c) M.Pedroni, F. Piccinelli, T. Passuello, M. Giarola, G. Mariotto, S. Polizzi, M. Bettinelli and A. Speghini *Nanoscale*, 2011, **3**, 1456-1460; (d) M. Yu, F. Li, Z. Chen, H. Hu, C. Zhan, H. Yang, C. Huang, *Anal. Chem.* 2009, **81**, 930–935; (e) Q. Liu, W. Feng, T. Yang, T. Yi, F. Li, *Nature Protocols* 2013, **8**, 2033–2044.
4. (a) D. K. Chatterjee, L. S. Fong, Y. Zhang, *Adv. Drug. Delivery Rev.* 2008, **60**, 1627-1637; (b) D. Yang, P. Ma, Z. Hou, Z. Cheng, C. Li, J. Lin, *Chem. Soc. Rev.* 2015, **44**, 1416-1448; (c) Y. Dai, D. Yang, P. A. Ma, X. Kang, X.;.Zhang, C. Li, Z. Hou, Z.; Cheng, J. Lin, J. *Biomaterials* 2012, **33**, 8704.
5. J-C. G. Bünzli, S. V. Eliseevaa, *Chem. Sci.* 2013, **4**, 1939-1949.
6. J. Pichaandi, J. C. Boyer, K. R. Delaney, F. C. J. M. van Veggel, *J. Phys. Chem.* 2011, **115**, 19054-19064.
7. D. K. Chatterjee, M. K. Gnanasammandhan, Y. Zhang, *Small* 2010, **24**, 2781-2795.
8. D. K. Chatteriee, A. J. Rufalhah, Y. Zhang, *Biomaterials* 2008, **29**, 937-943.
9. (a) N. M. Idris, Z. Q. Li, L. Ye, E. K. W. Sim, R. Mahendran, P. C. L. Ho, Y. Zhang, *Biomaterials* 2009, **30**, 5104-5113; (b) M. Priyam, N. M. Idris, Y. Zhang, *J. Mater. Chem.* 2012, **22**, 960-965.
10. S.Gai, C. Li, P. Yang, and J. Lin, *Chem. Rev.* 2014, **114**, 2343−2389.
11. F. Auzel, *Chem. Rev.* 2004, **104**, 139-173.
12. M. Haase, H. Schafer, *Angew. Chem. Int. Ed.* 2011, **50**, 5808-5829.
13. J. Wang, F. Wang, C. Wang, Z. Liu, X. Liu, *Angew. Chem. Int. Ed.* 2011, **50**, 10369-10372.
14. N. J. J. Johnson, N. M. Sangeetha, J.-C. Boyer, F. C. J. M. van Veggel, *Nanoscale* 2010, ***2*,** 771-777.
15. S. Sarkar, B. Meesaragandla, C. Hazra, V. Mahalingam, *Adv. Mater.,* 2013, **25**, 856-860.
16. S. V. Eliseevaa, J-C. G. Bünzli, *Chem. Soc. Rev.* 2010, **39**, 189-227.
17. B. Meesaragandla, V. N. K. B. Adusumalli, V. Mahalingam, *Langmuir* 2015, **31**, 5521–5528.
18. H. Schäfer, P. Ptacek, O. Zerzouf, M. Haase, *Adv. Funct. Mater*. 2008, **18**, 2913-2918.
19. K. U. Kumar, K. Linganna, S. S. Babu, F. Piccinelli, A. Speghini, M. Giarola, G. Mariotto, C. K. Jayasankar, *Sci. Adv. Mater*. 2012, **4**, 1-7.
20. J. Shan, Y. Ju, *Appl. Phys. Lett*. 2007, **91**, 123103.
21. H. X. Mai, Y. W. Zhang, L. D. Sun, C. H. Yan, *J. Phys. Chem. C* 2007, **111**, 13730–13739.
22. (a) Q. Liu, Y. Sun, C. Li, J. Zhou, C. Li, T. Yang, X. Zhang, T. Yi, D. Wu, F. Li, *ACS Nano* 2011, **5**, 3146–3157; (b) Y. Liu, M. Chen, T. Cao, Y. Sun, C. Li, Q. Liu, T. Yang, L.Yao, W. Feng, F. Li, *J. Am. Chem. Soc.* 2013, **135**, 9869−9876; (c) J. Zhou, Q. Liu, W. Feng, Y. Sun, F. Li, *Chem. Rev.* 2015, **115**, 395−465.
23. (a) Z. Chen, H. Chen, H. Hu, M. Yu, F. Li, Q. Zhang, Z. Zhou, T. Yi, C. Huang, *J. Am. Chem. Soc.* 2008, **130**, 3023-3029 (b) R. Naccache, F. Vetrone, V. Mahalingam, L. A. Cuccia, J. A. Capobianco, *Chem. Mater*. 2009, **21**, 717-723.
24. H. Hu, M. Yu, F. Li, Z. Chen, X. Gao, L. Xiong, C. Huang, *Chem. Mater*. 2008**, 20***,* 7003-7009.
25. B. Meesaragandla, S. Sarkar, C. Hazra, V. Mahalingam, *ChemPlusChem.* 2013**, 78,** 1338–1342.
26. (a) J. C. Boyer, F. Vetrone, L. A. Cuccia, J. A. Capobianco, *J. Am. Chem. Soc.* 2006, **128**, 7444–7445; (b) B. Meesaragandla, V. Mahalingam, *Chem. Eu. J*., 2015, **21**, 1-8.
27. V. Mahalingam, F. Vetrone, R. Naccache, A. Speghini, J. A. Capobianco, *Adv. Mater.* 2009, **21**, 4025–4028.
28. F. Wang, Y. Han, C. S. Lim, Y. Lu, J. Wang, J. Xu, H. Chen, C. Zhang, M. Hong and X. Liu, *Nature*, 2010, **463**, 1061–1065.
29. S. Sarkar, C. Hazra and V. Mahalingam, *Chem. Eu. J*., 2012, **18**, 7050-7054.
30. S. Sarkar, V. N. K. B. Adusumalli, V. Mahalingam, J. A. Capobianco, *Phys. Chem. Chem. Phys*. 2015, **17**, 17577–17583.
31. G. Chen, T. Y. Ohulchanskyy, R. Kumar, H. Ågren, P. N. Prasad, *ACS Nano*. 2010, **4**, 3163–3168.
32. W. D. Horrocks, D. R. Sudnick, *J. Am. Chem. Soc*. 1979, **101**, 334–340.